EUROMECH COLLOQUIUM 578
Rolling Contact Mechanics for Multibody System Dynamics
Funchal, Madeira, Portugal, April 10 to 13, 2017
J.Ambrósio, W.Schiehlen, J.Pombo (Editors)

OCCURRENCE AND REMOVAL OF WIGGLES IN TRANSIENT ROLLING CONTACT SIMULATION.

Cornelis D. van der Wekken[⋆†], Edwin A.H. Vollebregt[⋆], Kees Vuik[†]

[⋆]V$\mathcal{O}$Rtech BV
2600AG Delft, the Netherlands
niels.vanderwekken@vortech.nl, edwin.vollebregt@vortech.nl

[†]Delft Institute of Applied Mathematics, Delft University of Technology
Mekelweg 4, 2628CD Delft, the Netherlands
c.vuik@tudelft.nl

Keywords: rolling contact, wheel-rail, transient, multi-body dynamics, traction, instabilities.

Summary: *The CONTACT software created by Kalker and further developed by Vollebregt has recently been integrated in dynamical simulation software like RecurDyn and libraries usable in Matlab or C. When such larger packages impose small timesteps compared to the gridsize used, a wiggle-like phenomenon arises. Additionally, transient time-stepping appears to give rise to a smoothing effect that alters detailed traction profiles. A method is presented that focuses on scaling of the timestep for the influence coefficient matrices. This method stops the occurrence of wiggles. Furthermore, the smoothing effect is explained and a solution for this problem is proposed using world-fixed coordinates. These two refinements result in an improved algorithm that allows for small timesteps to be chosen in CONTACT, producing results consistent with results using larger timestep sizes.*

1. INTRODUCTION

A detailed model for wheel-rail rolling contact analysis is provided by Kalkers variational theory. This theory is provided by the CONTACT software [1, 2].

Recent developments by Vollebregt aim at integrating CONTACT into transient vehicle models. This application gives rise to the need of using a given timestep independent of the rolling velocity and gridsize. Unexpectedly, this causes a wiggle-like phenomenon to arise in the tangential traction profile. Unlike the situation in computational fluid dynamics, these wiggles appear when the timestep becomes small compared to the gridsize. This phenomenon is

grid-dependent and deviates from the Carter-Fromm solution for 2D steady state rolling, and is therefore clearly nonphysical.

Section 2 gives the necessary theoretical background for analyzing this problem. Then an explanation for the appearance of the wiggles is given in Section 3, together with a solution for this problem in Section 4. A second effect caused by the scaling of the timestep is explained in Section 5. A solution that solves this second effect is given in Section 6, after which we will draw our conclusions in Section 7.

2. THEORY

Kalker's variational theory is essentially a boundary element appoach. The main variables are the tractions $p^{(a)}$ acting on the surfaces $a = 1, 2$, and the displacements $u^{(a)}$ of the surface particles. Attention is focused on the traction $p := p^{(1)} = -p^{(2)}$ and on the displacement difference $u = u^{(1)} - u^{(2)}$. These are linked using analytical Boussinesq-Cerruti solutions, using the half-space approach [1].

In order to analyze the wiggles we focus on the tangential tractions and restrict ourselves to 2D transient scenarios. Next to this we consider only quasi-identical cases so that we have influence functions $A^{xz} = A^{zx} = 0$. This simplifies the influence functions because u_x only depends on p_x. Now the influence function works as follows:

$$u_x(x) = \int_C A^{xx}(x, y) p_x(y)\, dy. \tag{1}$$

This results in a scalar problem for $p := p_x$, $u := u_x$ and $s := s_x$, for a more detailed description see [3, 4]. The slip equations [1] are thus simplified to a scalar formulation:

$$s = w + \frac{\dot{u}}{V}, \tag{2}$$

where:

$$\text{in adhesion } H: \qquad |s| = 0, \quad |p| \leq g = \mu p_n, \tag{3}$$

$$\text{in slip } S: \qquad |s| > 0, \quad p = -g\frac{s}{|s|}. \tag{4}$$

2.1 Discretization of the problem

To find a numerical solution to the slip equations (2-4) CONTACT uses a cell centred rectangular discretization. We discretize equation (2) in time and indicate a time-discretised solution at time $t = dt \cdot i$ by u. A solution at the previous time $t' = t - dt$ will be adressed by u'.

CONTACT has two different strategies for dealing with the time-dependence. Using 'world-fixed' (shift) and 'moving coordinates' (rolling). The first is comparable to the Lagrangian (material fixed) approach, which is the more traditional approach in finite element analysis as described in the books by Wriggers [5] or Laursen [6]. The second is comparable to the

arbitrary Lagrangian Eulerian approach developed for rolling contact scenarios as used by Nackenhorst [7].

In the world fixed approach we have a single mesh. The tractions p and p' are approximated by a piecewise constant function, constant on each cell. The displacement differences u and u' (as well as the slip s, s') are determined only in the cell-centres.

The mesh in the moving coordinates approach is fixed to the contact area. This means that for each timestep the mesh shifts with respect to the contact particles by $dq = V \cdot dt$. In each step, new particles are being studied because the particles in cell n of the new mesh are not the same as the particles in cell n of the old mesh. The method needs u' at the centres of the new mesh in order to form the time derivative. This involves integrals of Ap' from cells of the new mesh to the cell centres of the new mesh.

The material derivative $\dot{u}$ can be discretized as:

$$\frac{Du}{Dt} \approx \frac{u(x(t)) - u'(x(t-dt))}{dt}. \tag{5}$$

This transforms the continuous slip equation into a time-discretized form:

$$s = w + \frac{1}{V}\frac{u(x(t)) - u'(x(t-dt))}{dt}. \tag{6}$$

Discretization in space will give us a grid of elements I. In the centre of element I we will keep track of the values of the traction p_I. The real traction p will be approximated by the use of constant basisfunctions $\phi_I(x)$ that are 1 inside one cell and zero everywhere else, so that we have $p(x) \approx \sum_I p_I \phi_I(x)$. This turns (6) into a space-discretized form:

$$s_I = w_I + \frac{u_I(x_I(t)) - u'_I(x_I(t-dt))}{V \cdot dt}. \tag{7}$$

The traversed distance per timestep $V \cdot dt$ will from now on be replaced by dq. Also note that if a particle is at position x_I at time t, then it was at position $x_I + V \cdot dt = x_I + dq$ at time $t - dt$ in a moving coordinate frame. So write x_I for x at the current time and x'_I for x at the previous timestep:

$$s_I = w_I + \frac{u_I(x_I) - u'_I(x'_I)}{dq}. \tag{8}$$

Now we have to replace the displacements by tractions using the relation given in equation (1). This can be done by discretizing the influence functions. The influence functions are discretized by calculating the displacements felt in element I as a result of tractions in element J. This means that influence coefficient A^{ij}_{IJ} indicates how the displacement in element I in the i direction is influenced by tractions in element J in the j direction. As we will only use variables in the x direction from here on write $A_{IJ} := A^{xx}_{IJ}$. The continuous operation (1) is now discretized to a matrix vector product $u(x_I) = A_{IJ}p_J$. To deal with u' we have to calculate

a slightly shifted set of influence coefficients, where we do not integrate over the contact area C at the current time, but have to integrate over the contact area C' at the previous time:

$$u'(x) = \int_{C'} A(x,y)p'(y)\,dy, \tag{9}$$

which gives us $u'_I = \sum_J A'_{IJ}p'_J$. This turns equation (8) into the system:

$$s_I = w_I + \sum_J \frac{A_{IJ}p_J - A'_{IJ}p'_J}{dq}. \tag{10}$$

Here we still have two unknowns s_I and p_I, to solve this problem we will go back on the contact conditions (3) and (4). These constraints allow us to either eliminate the slip or the traction as an unknown. Before we can do this we need to split the equation in a part that lives on the elements in the adhesion area and a part that lives on the elements that are in the slip area. Use the following notation:

$$\mathbf{p} = \begin{bmatrix} \mathbf{p_H} \\ \mathbf{p_S} \end{bmatrix}, \quad \mathbf{s} = \begin{bmatrix} \mathbf{s_H} \\ \mathbf{s_S} \end{bmatrix}, \quad \mathbf{w} = \begin{bmatrix} \mathbf{w_H} \\ \mathbf{w_S} \end{bmatrix}, \quad A = \begin{bmatrix} A_{HH} & A_{HS} \\ A_{SH} & A_{SS} \end{bmatrix}. \tag{11}$$

Now we can use (3) that simply tells us that $\mathbf{s_H} = \mathbf{0}$. In the slip area (4) tells us that $\mathbf{p_S}$ reaches the traction bound and should have the opposite sign from the slip $\mathbf{s_S}$. This turns equation (10) into:

$$\begin{bmatrix} \mathbf{0} \\ \mathbf{s_S} \end{bmatrix} = \begin{bmatrix} \mathbf{w_H} \\ \mathbf{w_S} \end{bmatrix} + \frac{1}{dq}\begin{bmatrix} A_{HH} & A_{HS} \\ A_{SH} & A_{SS} \end{bmatrix}\begin{bmatrix} \mathbf{p_H} \\ \mathbf{p_S} \end{bmatrix} - \frac{1}{dq}\begin{bmatrix} A'_{HH} & A'_{HS} \\ A'_{SH} & A'_{SS} \end{bmatrix}\begin{bmatrix} \mathbf{p'_H} \\ \mathbf{p'_S} \end{bmatrix}. \tag{12}$$

In the adhesion area the system can be written for $\mathbf{p_H}$ as:

$$\mathbf{p_H} = -{A_{HH}}^{-1}(\mathbf{w_H} + A_{HS}\mathbf{p_S} - A'_{HH}\mathbf{p'_H} - A'_{HS}\mathbf{p'_S}). \tag{13}$$

In the slip area the system for $\mathbf{p_S}$ turns into:

$$\mathbf{s_S} = \mathbf{w_S} + A_{SH}\mathbf{p_H} + A_{SS}\mathbf{p_S} - A'_{SH}\mathbf{p'_H} - A'_{SS}\mathbf{p'_S}, \tag{14}$$

Note that in the slip area the traction has reached the traction bound $g = \mu p_n$. Therefore we have $\mathbf{p_S} = \pm\mu\mathbf{p_n}$, which a known and thus no longer a variable in the equations. On top of this $\mathbf{p_S}$ and $\mathbf{p'_S}$ are equal when the sign of the slip does not change between the time instances. We can then group the two terms and get the contribution $(A_{SS} - A'_{SS})\mathbf{p_S}$.

The key feature of equation (13) is that there is a matrix $(A^{-1}_{HH}A'_{HH})$ that shows how the next solution $\mathbf{p_H}$ is a function of the previous solution $\mathbf{p'_H}$ plus some shift caused by the slip area.

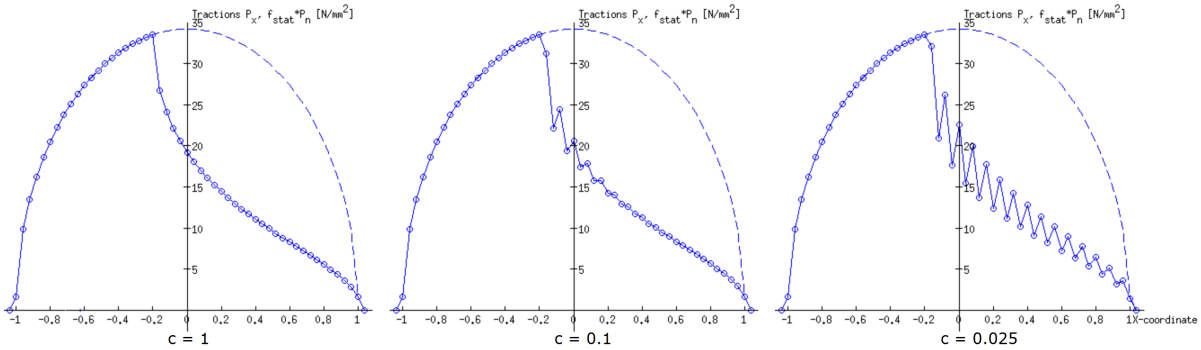

Figure 1. Computations of tractions in 2D in CONTACT choosing different values of c. This is the 2D Carter/Fromm problem, see [2, Section 5.2]. The full line is the p_x traction profile, the dashed line is the traction bound.

3. WIGGLES FOR SMALL TIMESTEPS

Problems arise when the factor $c = \frac{dq}{dx}$ becomes small, an example of the wiggles that appear at small values of c is given in Figure 1. This example is from a steady-state rolling computation. During transient rolling the same behaviour is observed, where the wiggles start small and accumulate over time giving the same long-term result.

Physically a small c means that the traversed distance per timestep is small compared to the gridsize. Mathematically this means that the discretized influence coefficients A and A' become increasingly similar.

A simple solution to this is never choosing a too small factor c. This is a nice solution when only running the program CONTACT by itself, however CONTACT has been integrated in larger multi-body simulation packages, in such cases the input parameters by CONTACT are no longer handpicked but fed to the software by the overall package. This is why we want to improve the method so that CONTACT can be adjusted and it converges properly for any value of c.

3.1 Reason why wiggles appear

To explain the origin of the wiggles for small c we look back at equation (13). Here the matrix $A - A'$ plays a role. Figure 2 shows that the inverse of $A - A'$ behaves nicely for $c = 1$, now if we decrease c far enough ripples on the sides its inverse appear, and for $c = 0.01$ the result is shown in Figure 3.

As can be seen in Figure 3, when c becomes small the values on the diagonal of A become close to zero compared to the rest of the rest of the matrix. One might think that using higher order basisfunctions to construct the matrix A would solve this problem. We have analytically constructed the influence coefficients based on bilinear basisfunctions to try this. No improvement has been observed however. The behaviour observed in Figure 3 stays the same when using higher order basisfunctions for the construction of A.

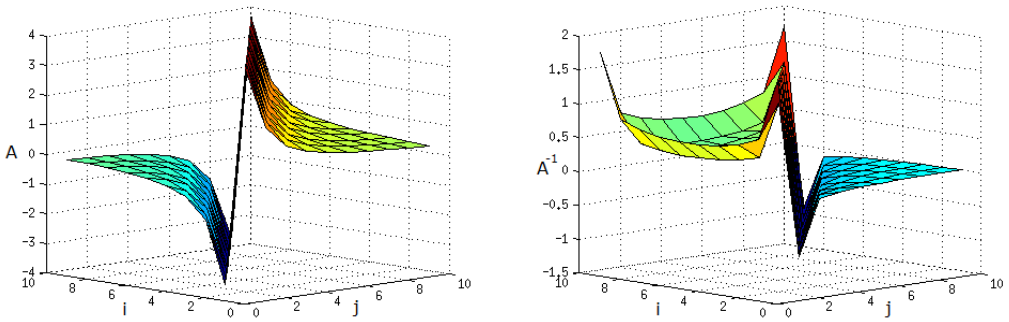

Figure 2. Matrix $A - A'$ (left) and its inverse (right) for $c = 1$.

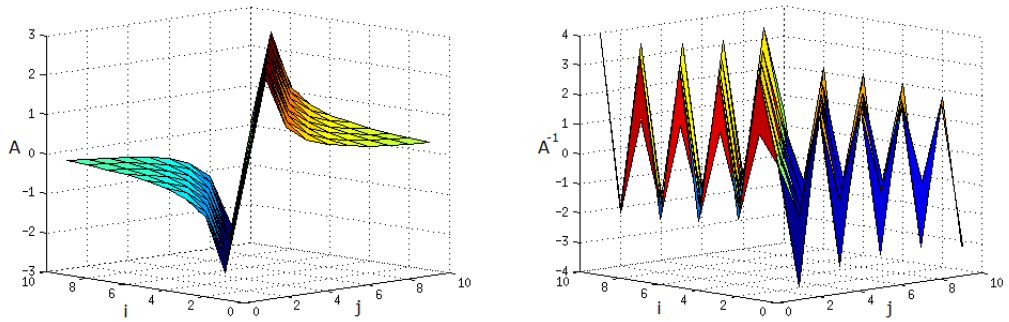

Figure 3. Matrix $A - A'$ (left) and its inverse (right) for $c = 0.01$.

This erratic behaviour of the inverse can be explained when we approximate the inverse of $A - A'$ by using Fast Fourier Transformations. This approximation can be done because $A - A'$ is a Toeplitz matrix, see Vollebregt [8] for this procedure. When we apply this method it turns out that for $c = 1$ all frequencies in the frequency domaim are of similar size. When we do the same for $c \downarrow 0$ the high frequencies dominate the frequency domain, which results in the undesirable behaviour of the solution.

4. TIME-STEPPING ADJUSTMENT

In Section 3 we have concluded that it is unfavourable to directly calculate the influence coefficients when using a small value of c. This brings us to the application of interpolation. Assume that the influence coefficients behave as a linear function of c around the origin and write:

$$A'(c) \approx \left(1 - \frac{c}{c^*}\right) A'(0) + \frac{c}{c^*} A'(c^*). \tag{15}$$

Here $A'(\xi)$ is the influence coefficient matrix A calculated as in (9) where the area of integration is shifted over a distance ξ. For clarity, note that $A'(0)$ is just A. Instead of directly calculating the influence coefficients $A'(c)$ for the needed c we can now calculate the influence coefficients $A'(c^*)$ for a sufficiently large c^* and approximate $A'(c)$ using this alternative $A'(c^*)$.

4.1 Interpolation of A'

Now call the ratio of c over c^* the interpolation parameter $\theta = \frac{c}{c^*}$. We will write for the coefficient matrix calculated with the larger timestep using c^* the matrix A^*. The new matrix A', calculated using the interpolation parameter θ and the matrix A and A^* now becomes:

$$A' = (1 - \theta)A + \theta A^*. \tag{16}$$

The problems arose when we started working with the inverse of $A - A'$ for a small value of c. Now however $A - A'$ becomes $A - ((1 - \theta)A + \theta A^*) = \theta(A - A^*)$. Where the quantity $A - A^*$ behaves nicely, also inversed, because we can choose c^* large enough.

Figure 4 shows the results using interpolation. These results were generated in Matlab for the 2D Cattaneo to Carter testcase [2, example 5.8]. This shows that the wiggles are suppressed effectively by the interpolation of $A'(c)$. However, a new feature in the results is the appearance of smoothing or numerical diffusion.

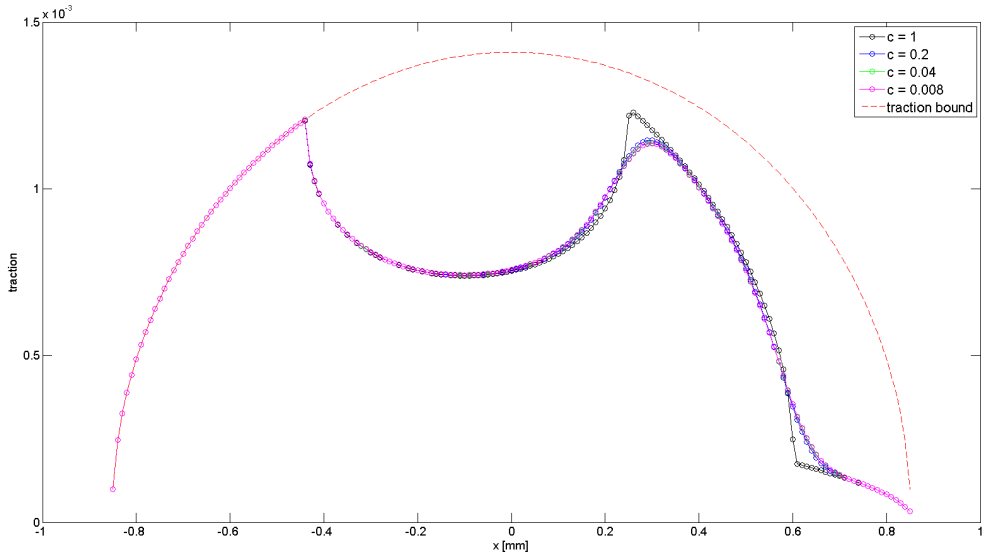

Figure 4. Results of the new method for a transient simulation (Cattaneo to Carter scenario), after a traversed distance of $24\Delta x$, using different values of c.

5. SMOOTHING EFFECTS

When we apply interpolation of $A'(c)$ in the calculation, the first observation is that indeed there appear no artificial wiggles. The second observation however is that solutions obtained with $c < 1$ stay near the solution found using $c = 1$ in a big part of the domain, but deviate from the solution around sharp edges. In Figure 4 this can be observed at the bends around $x = 0.3$ and $x = 0.6$.

5.1 Reason why smoothing effects occur

The appearance of this deviation from the original solution ($c = 1$), which looks like suppression of extrema, has the characteristics of numerical diffusion. Looking back at the original CONTACT program we see the same smoothing effect at values of c in the range $0.9-0.6$ where no wiggles are found.

Altough the problem with wiggles only occurs for small values of c, the effects of smoothing appear for any non-integer value of c. At first this is an unexpected effect, as the analytical influence coefficients should in theory result in a correct solution. To investigate this subject we will go back to equations (13). Remember that the matrix ${A_{HH}}^{-1}A'_{HH}$ says how the old solution is carried over to a new position. Here take a closer look at what ${A_{HH}}^{-1}A'_{HH}$ exactly does to $\mathbf{p'_H}$. This is easiest done by looking at what happens to a traction that has the value one at a single place and is zero everywhere else. If we know what happens to such a traction we know what happens to a realistic traction profile.

When looking at the matrix ${A_{HH}}^{-1}A'_{HH}$, multiplying this with a vector with a one at the i^{th} position and zeros everywhere else results in the i^{th} column of the matrix. When using $c = 1$ this matrix has, except for the first column, a one on the $(i-1)^{th}$ position and zeros everywhere else. For $c = 0$ the matrix is just the identity matrix because then $A' = A$. For $0 < c < 1$ however, the columns of ${A_{HH}}^{-1}A'_{HH}$ have non-zero values in multiple rows, this means that the traction with a non-zero value at a single point in space becomes smeared out after the first transformation. Repetitive iterations only increase this effect.

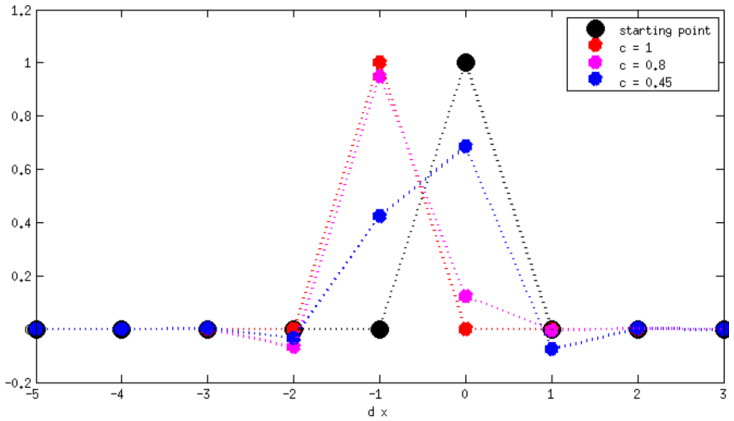

Figure 5. Illustration of the smothing effect for different c. Using $c = 1$, the initial traction (black) is shifted precisely one grid cell, whereas with $c < 1$, the value is distributed over different points.

Figure 5 shows how ${A_{HH}}^{-1}A'_{HH}$ transforms a p'_H that is one at $x_I = 0$ and zero everywhere else after one timestep. We see that in the case $c = 1$ this transformation is nothing but a horizontal translation over one gridpoint. This behaviour is desired for all c. However, for $c < 1$ it is impossible to have this result as there are no gridpoints between 0 and $-\Delta x$. Instead the result is a transformation that puts the weight of the new p_H in between 0 and $-\Delta x$. The

columns of ${A_{HH}}^{-1}A'_{HH}$ sum up to one for all c so the total traction does stay constant in all cases.

If we apply the time-stepping adjustment from Section 4 the effect of smoothing is not resolved, not even when using $c^* = 1$. When using $c^* = 1$ we use a matrix A^* where $\delta q^* = \delta x$. The equation for the traction in adhesion takes the following form:

$$p_{J1} = \delta q A^{-1}_{I1J1} \left(-w_I + \frac{A'_{I1J1}}{\delta q} p'_{J1} \right). \tag{17}$$

Now we can substitute in equation (17) our approximation for A' as given by (16). This results in the following equation for the traction, where $\delta q = c\delta x$ and $\delta q^* = c^*\delta x$:

$$\begin{aligned}
p &= \delta q A^{-1} \left(-w + \frac{A'}{\delta q} p' \right) && (18)\\
&= \delta q A^{-1} \left(-w + \left((1-\theta)\frac{A}{\delta q} + \theta \frac{A^*}{\delta q} \right) p' \right) && (19)\\
&= \delta q A^{-1} \left(-w + (1-\theta)\frac{A}{\delta q} p' + \theta \frac{A^*}{\delta q} p' \right) && (20)\\
&= -\delta q A^{-1} w + (1-\theta)\delta q A^{-1} \frac{A}{\delta q} p' + \theta \delta q A^{-1} \frac{A^*}{\delta q} p' && (21)\\
&= -\delta q A^{-1} w + (1-\theta) p' + \theta \delta q A^{-1} \frac{A^*}{\delta q} p' && (22)\\
&= (1-\theta) p' + \delta q A^{-1} \left(-w + \theta \frac{A^*}{\delta q} p' \right) && (23)\\
&= (1-\theta) p' + \theta \delta q^* A^{-1} \left(-w + \frac{A^*}{\delta q^*} p' \right) && (24)\\
&= (1-\theta) p' + \theta p^* && (25)
\end{aligned}$$

In the last but one step we used that: $\delta q = c\delta x$ and $\theta = \frac{c}{c^*}$. So we can write $\delta q = \frac{c}{c^*} c^* \delta x = \theta \delta q^*$ and $\frac{\theta}{\delta q} = \frac{c}{c^* c \delta x} = \frac{1}{\delta q^*}$. The p^* we introduced in (25) is what the new solution of p would be if instead of using c and a timestep δq we just used c^* and timestep δq^*.

The reason that interpolation of $A'(c)$ using a matrix A^* that was constructed with $c^* = 1$ still produces smoothing can be explained by looking at the interpolation process in the way of equation (25). This says that the solution p is constructed as a weighted average of the solution p' at the previous timestep and the solution p^* of a point ahead in time (ahead by a factor θ^{-1}). So even if we not directly use the operator $A^{-1}A'$ we still get the same effect as illustrated in Figure 5. This means that a sharp point in the traction profile, like the peak around $x = 0.3$ in Figure 4, is updated at the new timestep by the average of two sharp profiles. This averaging will slightly flatten out the sharp point. The transient character of the problem will make sure that as we progress in time the flattening accumulates, smoothing out the sharp point completely.

In Figure 4 we see one sharp point in the solution that stays intact. This is because here the solution moves into the traction bound, so altough averaging does still occur the averaging happens beyond the traction bound, and is thus cut off by the solver.

6. WORLD FIXED IMPLEMENTATION

Previously we looked at the contact problem in a contact fixed framework, the 'moving coordinates'. The motivation for this approach is that the grid moves along with the contact area such that the grid only has to be as large as the contact area. On the contrary, the world-fixed coordinates need a mesh that encompasses the whole distance traversed. For short simulations this is not a real issue, but when doing simulations where the total displacement covers a (large) multiple of the contact area this can be a problem.

The key difference between the two situations is that in the contact-fixed approach we have traction p_I at position x_I and want to move that traction to somewhere in between position x_{I-1} and x_I, while in a world-fixed approach we have traction p_I at position x_I and need to calculate a new traction in the next timestep, still at position x_I.

A simulation using the world-fixed approach had been performed with $c = 0.2$, the result can be found in Figure 6. This result shows that using a world fixed coordinate system preserves

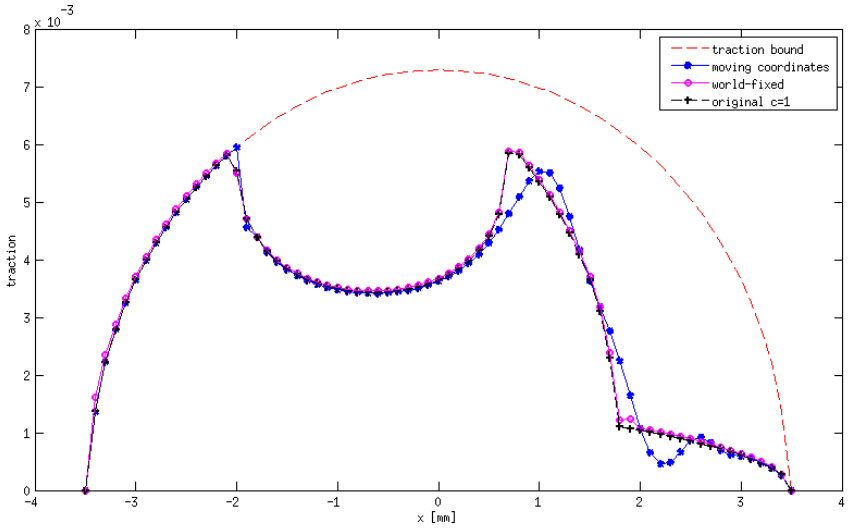

Figure 6. Results of a transient simulation (Cattaneo to Carter scenario). The moving coordinates (blue) and word-fixed simulation (magenta) were performed using $c = 0.2$. As a reference the black line shows the solution using moving-coordinates with $c = 1$. Shown situation is after a traversed distance of $17\Delta x$ in all cases.

the extrema in the traction profile. This gives solutions when using small values for c that are consistent with the solutions obtained for $c = 1$ using the current version of CONTACT.

In the current version of CONTACT, the world-fixed approach uses a grid that is the same during the whole simulation. This requires a grid that encompasses the whole distance traversed, which may be large, adversely affecting calculation time and memory usage. However, this is

only due to the implementation chosen, it is not a fundamental issue. There is still only a small region of interest in each time step. It is well possible to consider a small section of the overall grid in each time step, like a window moving over the rail, avoiding excessive calculations and memory use. This needs to be implemented.

7. CONCLUSIONS

In this paper two problems have been investigated and solutions have been given to solve both. The first problem is the appearance of wiggles arising when small time steps are used. This was caused by the amplification of high frequencies by the operator dealing with the spatial derivative in the slip-equation. An adjustment to the time-stepping scheme, using interpolation, is able to remove the wiggles, even at very small time steps.

Secondly, when using moving coordinates the original scheme as well as the one improved by the new time-stepping suffered from numerical smoothing of extrema in the solution. The use of a world-fixed implementation in stead of a contact-fixed implementation solves this problem. This comes down to looking at the problem in an Eulerian frame of reference (static) in stead of the previously more used Lagrangian frame of reference (moving camera).

References

[1] J.J. Kalker. *Three-Dimensional Elastic Bodies in Rolling Contact*. Solid Mechanics and its Applications. Kluwer Academic Publishers, Dordrecht, Netherlands, 1990.

[2] E.A.H. Vollebregt. User guide for CONTACT, Rolling and sliding contact with friction. Technical Report TR09-03, version 16.1, V$\mathcal{O}$Rtech, 2016. See `www.kalkersoftware.org`.

[3] E.A.H. Vollebregt and P. Wilders. FASTSIM2: a second order accurate frictional rolling contact algorithm. *Comput.Mech.*, 47(1):105–116, 2010.

[4] J. Zhao, E.A.H. Vollebregt, and C.W. Oosterlee. A fast nonlinear conjugate gradient based method for 3D concentrated frictional contact problems. *Journal of Computational Physics*, 288:86–100, 2015.

[5] P. Wriggers. *Computational Contact Mechanics, 2nd ed.* Springer, Heidelberg, 2006.

[6] T.A. Laursen. *Computational Contact and Impact Mechanics, Fundamentals of Modeling Interfacial Phenomena in Nonlinear Finite Element Analysis*. Springer, Berlin, 2002.

[7] U. Nackenhorst. The ALE-formulation of bodies in rolling contact - Theoretical foundations and finite element approach. *Comp. Meth. Appl. Mech. Eng.*, 193:4299–4322, 2004.

[8] E.A.H. Vollebregt. A new solver for the elastic normal contact problem using conjugate gradients, deflation, and an FFT-based preconditioner. *J. of Computational Physics*, 257, Part A:333–351, 2014.